Two-dimensional Angles Estimation Method and Its Improved Methods for Single Source with a Sparse Array

Jia-Jia Jiang[*], Fa-Jie Duan, Yan-Chao Li, and Xiang-Ning Hua

Abstract—Based on two orthogonal linear sparse arrays (LSA) which consist of the coupled-sensors (CSs), a high resolution and no ambiguity (HRNA) method is proposed to estimate the two-dimensional (2D) angles of single source. The HRNA method first constructs a new covariance matrix to achieve no ambiguity *independent* angles estimation by using the covariance matrix generated by each LSA, and then computes *joint* elevation and azimuth angles by utilizing both the estimated *independent* angles and triangular relationship. For large array aperture of the LSA, the HRNA method earns a high angle resolution; however, its *independent* angles estimation accuracy is slightly lower than the multiple signal classification (MUSIC) with a uniform linear array (ULA). In order to enhance the *independent* angle estimation performance, first improved HRNA (FI-HRNA) method is developed based on the HRNA and MUSIC methods. Further, in order to decrease the computational cost, second improved HRNA (SI-HRNA) method is presented based on FI-HRNA and MUSIC methods. The proposed SI-HRNA method obtains high angle resolution, high angle estimation accuracy and low computational load. In addition, the spacing between two adjacent CSs is not limited, and thus the angle resolution and estimation accuracy can be set according to practical demand. Numerical experiment and comparison with the other existing algorithms verify the effectiveness and superior performance of the method proposed in this paper.

1. INTRODUCTION

Single source localization is one of the most important topics in the speech localization [1], mobile phones localization [2–4], GPS localization [5], many radar systems [6], etc. Many relevant near-field (NF) and far-field (FF) source localization algorithms [1–17] for single source have been developed recently, such as these algorithms [2–5, 7–11] for NF single source and those [1, 12–17] for FF single source. For the NF single source localization, Cheung et al. [2] proposed a least squares algorithm to estimate the three-dimensional coordinate of single source, however, this algorithm requires a sufficiently high signal-to-noise ratio (SNR) condition in order to obtain a good estimation performance. In the process of solving the single source localization, an enhanced least squares method is presented in [3]. A circle fitting method in [5] is developed to achieve the GPS localization. Doroslovacki and Larsson [7] study different antenna placements issue in non-uniform linear arrays for the joint estimation of the range and direction of arrival (DOA), and some useful conclusions are provided. In addition, [8–11] also give some beneficial conclusions about NF single source localization.

For the FF single source angle estimation, a computationally efficient algorithm is presented to estimate the 2D angles with a uniform circle array in [12], and it is based on an assumption that the number of the sensors is even. Later on, another improved algorithm [13] is proposed to overcome the deficiency of the algorithm in [12]. However, these two algorithms in [12, 13] are only able to be used in uniform circle array and need extra method to solve the phase ambiguity issue. In [14], a single source DOA estimation algorithm, based on the second-order- statistic, is developed; in spite of using a

ULA, this algorithm still requires a complex process of solving the phase ambiguity. In [15], Bianchi et al. make a detailed statistical analysis for single source detection using random matrix theory. In [17], a novel algorithm is proposed to estimate the 2D angles of linear frequency-modulated signal, but it strongly depends on the type of source.

In this paper, we present a HRNA method for single source 2D angles estimation and then propose two improved methods (FI-HRNA and SI-HRNA methods) to enhance the angle estimation performance and decrease the computational complexity. Firstly, the proposed methods are based on two special LSAs, and note that the LSA consists of several CSs and the spacing between CSs can be set to very large according to both the large array aperture demand and high angle resolution request further. Secondly, although the LSA with large array aperture is used, the HRNA method can automatically solve the phase ambiguity problem. Thirdly, compared with the proposed HRNA method, the first improved method, FI-HRNA, gains a better angle estimation performance, and it is even more remarkable that its angle estimation accuracy can be improved continually as the array aperture increases constantly. Finally, the second improved method, SI-HRNA, inherits the merits of the FI-HRNA method, overcome the shortcoming of computational load, and thus has high angle estimation performance, high angle resolution and low computational cost.

2. PROBLEM FORMULATION

2.1. Review of Data Model of ULA

A ULA is composed of N sensors (see Fig. 1). The inter-sensor spacing is d. Assume one narrow-band source from FF impinging on this ULA from DOA ϕ_r.

The ULA output $\mathbf{x}(t) = [x_1, x_2, \ldots, x_N]^T$ can be modeled as

$$\mathbf{x}(t) = \mathbf{a}(\phi)s(t) + \mathbf{n}(t) \tag{1}$$

where $\mathbf{a}(\phi) = [a_1(\phi), a_2(\phi), \ldots, a_N(\phi)]^T = [1, e^{j\Omega}, \ldots, e^{j(N-1)\Omega}]^T$, $\mathbf{n}(t) = [n_1(t), n_2(t), \ldots, n_N(t)]^T$, $s(t)$ is a source, $n_i(t)$ is the noise in the i-th sensor, and $\Omega = [-2\pi d \cos\phi/\lambda]$, where λ is the wavelength of source and $\phi \in (0, \pi]$ [18]. T denotes the transpose. The covariance matrix $\mathbf{R}_1$ of this ULA is then given by

$$\mathbf{R}_1 = E\left\{\mathbf{x}(t)\mathbf{x}^H(t)\right\} = \sigma_s \mathbf{a}(\phi)\mathbf{a}^H(\phi) + \sigma_n \mathbf{I} = \begin{bmatrix} \sigma_s + \sigma_n & \sigma_s e^{-j\Omega} & \sigma_s e^{-j2\Omega} & \ldots & \sigma_s e^{-j(N-1)\Omega} \\ \sigma_s e^{j\Omega} & \sigma_s + \sigma_n & \sigma_s e^{-j\Omega} & \ldots & \sigma_s e^{-j(N-2)\Omega} \\ \sigma_s e^{j2\Omega} & \sigma_s e^{j\Omega} & \sigma_s + \sigma_n & \ldots & \sigma_s e^{-j(N-3)\Omega} \\ \vdots & \vdots & \vdots & \ddots & \vdots \\ \sigma_s e^{j(N-1)\Omega} & \sigma_s e^{j(N-2)\Omega} & \sigma_s e^{j\Omega} & \ldots & \sigma_s + \sigma_n \end{bmatrix} \tag{2}$$

where σ_s is the signal power, σ_n the noise variance, and H the conjugate transpose.
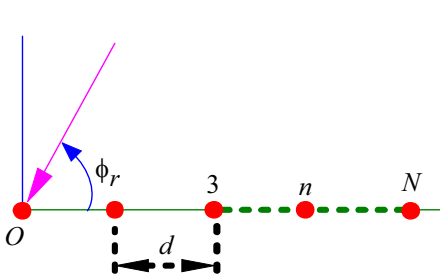

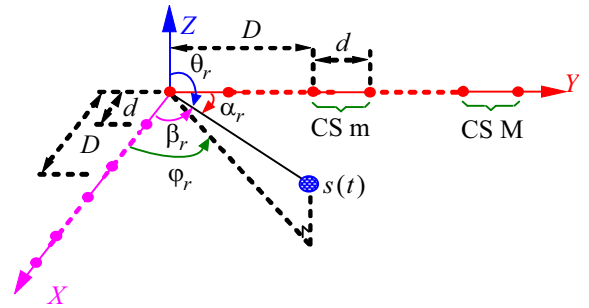**Figure 1.** The ULA configuration.

Figure 2. The two orthogonal linear sparse array configuration.

2.2. Data Model of Two Orthogonal LSAs

The array is composed of two orthogonal LSAs, and each LSA consists of M CSs as shown in Fig. 2. The inter-sensor spacing of CS is d, and inter-sensor spacing between CSs is D with $D = kd$ (k is a positive integer and $k \geq 3$ for a LSA). Single narrow-band source from FF impinges on two LSAs from *independent* angles α_r, $\alpha_r \in (0, \pi]$ and β_r, $\beta_r \in (0, \pi]$, respectively. Note that for convenience, the sensor on the left of the m-th CS on the Y axis is called CS_{m_1}, and one on the right of the m-th CS is called CS_{m_2}.

The LSA output $\mathbf{y}(t) = [y_1, y_2, \ldots, y_{2M-1}, y_{2M}]^T$ on the Y axis can be modeled as

$$\mathbf{y}(t) = \mathbf{b}(\alpha)s(t) + \mathbf{e}(t) \tag{3}$$

where $\mathbf{b}(\alpha) = [b_1(\alpha), b_2(\alpha), \ldots, b_{2M-1}(\alpha), b_{2M}(\alpha)]^T = [1, e^{j\Phi}, \ldots, e^{j[k(M-1)]\Phi}, e^{j[k(M-1)+1]\Phi}]^T$, $\Phi = [-2\pi d \cos \alpha / \lambda]$, $\mathbf{e}(t) = [e_1(t), e_2(t), \ldots, e_{2M-1}(t), e_{2M}(t)]^T$, and $e_i(t)$ is the noise in the i-th sensor.

The covariance matrix of this LSA on the Y axis is then given by

$$\mathbf{R}_y = E\left\{\mathbf{y}(t)\mathbf{y}^H(t)\right\} = \sigma_s^2 \mathbf{b}(\alpha)\mathbf{b}^H(\alpha) + \sigma_n^2 \mathbf{I}$$

$$= \begin{bmatrix} \sigma_s + \sigma_n & \sigma_s e^{-j\Phi} & \sigma_s e^{-jk\Phi} & \ldots & \sigma_s e^{-j[(M-1)k+1]\Phi} \\ \sigma_s e^{j\Phi} & \sigma_s + \sigma_n & \sigma_s e^{-j(k-1)\Phi} & \ldots & \sigma_s e^{-j(M-1)k\Phi} \\ \sigma_s e^{jk\Phi} & \sigma_s e^{j(k-1)\Phi} & \sigma_s + \sigma_n & \ldots & \sigma_s e^{-j[(M-2)k+1]\Phi} \\ \vdots & \vdots & \vdots & \ddots & \vdots \\ \sigma_s e^{j[(M-1)k+1]\Phi} & \sigma_s e^{j(M-1)k\Phi} & \sigma_s e^{j[(M-2)k+1]\Phi} & \ldots & \sigma_s + \sigma_n \end{bmatrix} \tag{4}$$

Throughout the paper, the following hypotheses are assumed to hold: 1) The incoming source signal is narrow-band, zero-mean complex Gaussian random processes; 2) The noise is zero-mean, complex circular Gaussian, and spatially uniformly white random processes, and is statistically independent of the source signal; 3) The inter-sensor spacing d of each CS satisfies $d \leq \lambda/2$; 4) The inter-sensor spacing between CSs D satisfies $D = kd$, and k is a positive integer and more that 2 for a LSA.

2.3. Joint 2D Angles and Angle Ambiguity

On the one hand, the relationship between array configuration for *independent* and *joint* 2D angles estimation is illustrated by [19]

$$\begin{cases} \sin \theta_r \sin \varphi_r = \cos \alpha_r \\ \sin \theta_r \cos \varphi_r = \cos \beta_r \end{cases} \tag{5}$$

where θ_r and φ_r denote the elevation and azimuth angles, respectively.

On the other hand, when there exists one source from angle α_r (β_r), several angle estimates, which contain one real and multiple false angle estimates, can be obtained by utilizing the MUSIC method in [18] to the LSA on the Y (X) axis, which indicates there exists angle ambiguity when the LSA is used. Fig. 3 gives an example of angle ambiguity. In this experiment, the LSA on the Y axis in Fig. 2 and a ULA are used, M is set to 3, the input signal-to-noise ratio (SNR) of source is 0 dB, the *independent* angle α_r of source is 10°, and the number of snapshots is 1000.

Therefore, from the relationship for *independent* and *joint* 2D angles, one can see that, in order to obtain the *joint* elevation and azimuth angles, we need to estimate **no ambiguity** *independent* angles α_r and β_r.

3. PROPOSED METHOD

In order to remove the angle ambiguity issue and then obtain right and *independent* angles estimates, we propose the following HRNA method. First of all, $\mathbf{R}_2$ can be obtained from $\mathbf{R}_1$ as [18]

$$\mathbf{R}_2 = \mathbf{R}_1 - \mathrm{diag}(\sigma_n) = \sigma_s \mathbf{a}(\phi)\mathbf{a}^H(\phi) = \begin{bmatrix} \sigma_s & \sigma_s e^{-j\Omega} & \sigma_s e^{-j2\Omega} & \ldots & \sigma_s e^{-j(N-1)\Omega} \\ \sigma_s e^{j\Omega} & \sigma_s & \sigma_s e^{-j\Omega} & \ldots & \sigma_s e^{-j(N-2)\Omega} \\ \sigma_s e^{j2\Omega} & \sigma_s e^{j\Omega} & \sigma_s & \ldots & \sigma_s e^{-j(N-3)\Omega} \\ \vdots & \vdots & \vdots & \ddots & \vdots \\ \sigma_s e^{j(N-1)\Omega} & \sigma_s e^{j(N-2)\Omega} & \sigma_s e^{j\Omega} & \ldots & \sigma_s \end{bmatrix} \tag{6}$$

where σ_n can be estimated through $\hat{\sigma}_n = \frac{1}{N-1}\sum_{n=1}^{N-1}\lambda_n$ [20], λ_n denotes the n-th smallest eigenvalue of the matrix $\mathbf{R}_1$. Likewise, $\bar{\mathbf{R}}_y$ can be obtained from $\mathbf{R}_y$ as

$$
\begin{aligned}
\bar{\mathbf{R}}_y &= \mathbf{R}_y - \text{diag}(\sigma_n) = \sigma_s^2\mathbf{b}(\alpha)\mathbf{b}^H(\alpha) \\
&= \begin{bmatrix}
\sigma_s & \sigma_s e^{-j\Phi} & \sigma_s e^{-jk\Phi} & \cdots & \sigma_s e^{-j[(M-1)k+1]\Phi} \\
\sigma_s e^{j\Phi} & \sigma_s & \sigma_s e^{-j(k-1)\Phi} & \cdots & \sigma_s e^{-j(M-1)k\Phi} \\
\sigma_s e^{jk\Phi} & \sigma_s e^{j(k-1)\Phi} & \sigma_s & \cdots & \sigma_s e^{-j[(M-2)k+1]\Phi} \\
\vdots & \vdots & \vdots & \ddots & \vdots \\
\sigma_s e^{j[(M-1)k+1]\Phi} & \sigma_s e^{j(M-1)k\Phi} & \sigma_s e^{j[(M-2)k+1]\Phi} & \cdots & \sigma_s
\end{bmatrix}
\end{aligned}
\tag{7}
$$

where σ_n can be estimated through $\hat{\sigma}_n = \frac{1}{2M-1}\sum_{m=1}^{2M-1}\lambda_m$ [20], λ_m is the m-th smallest eigenvalue of the matrix $\mathbf{R}_y$ and diag$\{\cdot\}$ defines a diagonal matrix. From (6), one can observe the following relationship:

$$
R_2(m,i)/R_2(m-1,i) = e^{j\Omega} \tag{8}
$$

where $R_2(m, i)$ denotes the (m, i)-th element of the matrix $\mathbf{R}_2$. And the matrix $\mathbf{R}_2$ is a Hermitain Toeplitz matrix [18], while the matrix $\bar{\mathbf{R}}_y$ has not a Hermitain Toeplitz structure characteristic.

If directly using the matrix $\mathbf{R}_y$ or $\bar{\mathbf{R}}_y$ to perform the MUSIC method for angle estimation, the angle ambiguity problem can be not overcome, which has been proved in Fig. 3. Therefore, in the following, by utilizing the special characteristic denoted by (6), which ensures there is no angle ambiguity, we will construct a new matrix $\mathbf{R}_{Ty}$ to let it have the same matrix structure as the matrix $\mathbf{R}_2$, to overcome the angle ambiguity problem.

We construct a new vector $\mathbf{z} = [z_1, z_2, \ldots, z_{(M-1)k+1}]^T$, and define the following relationship:

$$
z_1 = \hat{\sigma}_s = \frac{1}{2M}\sum_{i=1}^{2M}\bar{R}_y(i,i), \quad i = 1, 2, \ldots, 2M \tag{9}
$$

$$
z_q = z_1\rho^{q-1}, \quad q = 2, 3, \ldots, (M-1)k+2 \tag{10}
$$

$$
\rho = \frac{1}{2M^2}\sum_{i=1}^{2M}\sum_{m=1}^{M}R_4(2m,i)/R_4(2m-1,i) \tag{11}
$$

where $\bar{R}_y(m, i)$ is the (m, i)-th element of the matrix $\bar{\mathbf{R}}_y$. Note that one can observe from (11) that ρ denotes an estimate of $e^{j\Phi}$. Then we construct a $[(M-1)k+2] \times [(M-1)k+2]$ Toeplitz matrix $\mathbf{R}_{Ty}$
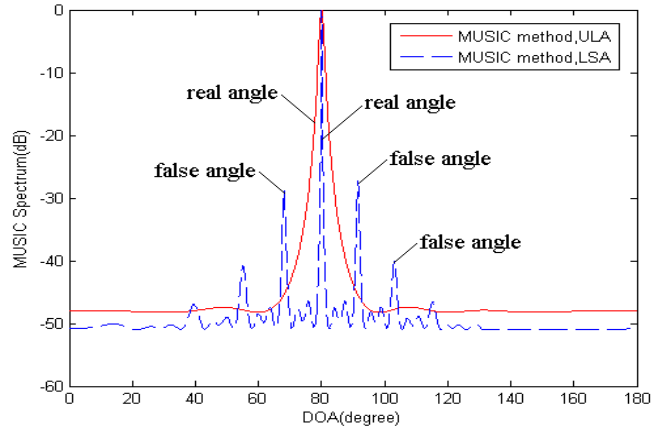

Figure 3. The MUSIC spectrum versus both the LSA and ULA.

whose first column and row are $\mathbf{z}$ and $\mathbf{z}^H$, respectively

$$\mathbf{R}_{Ty} = \begin{bmatrix} z_1 & z_2^* & \cdots & z_{(M-1)k+2}^* \\ z_2 & z_1 & \ddots & \vdots \\ \vdots & \cdots & \ddots & z_2^* \\ z_{(M-1)k+2} & \cdots & z_2 & z_1 \end{bmatrix} = \begin{bmatrix} z_1 & z_1\rho^{-1} & \cdots & z_1\rho^{-[(M-1)k+1]} \\ z_1\rho & z_1 & \ddots & \vdots \\ \vdots & \cdots & \ddots & z_1\rho^{-1} \\ z_1\rho^{[(M-1)k+1]} & \cdots & z_1\rho & z_1 \end{bmatrix} \quad (12)$$

From $\mathbf{R}_{Ty}$, one can find the following relationship like (8)

$$R_{Ty}(m,i)/R_{Ty}(m-1,i) = e^{j\Phi} \quad (13)$$

where $R_{Ty}(m,i)$ denotes the (m,i)-th element of the matrix $\mathbf{R}_{Ty}$. Comparing (12), (13) and (6), (8), one can find that $\mathbf{R}_{Ty}$ has the same characteristic as $\mathbf{R}_2$ and can be given by (14), and thus we can use $\mathbf{R}_{Ty}$ to obtain no ambiguity and *independent* angle estimation.

$$\mathbf{R}_{Ty} = \hat{\sigma}_s \mathbf{c}(\theta)\mathbf{c}^H(\theta) \quad (14)$$

where $\mathbf{c}(\theta) = [1, \rho, \rho^2, \ldots, \rho^{[(M-1)k+1]}]^T$.

In fact, the matrix $\mathbf{R}_{Ty}$ can be considered as a covariance-like, which is generated by a special ULA. And this special ULA is composed of both real CSs and fictitious sensors between real CSs. Therefore, based on $\mathbf{R}_{Ty}$ and using the MUSIC [18] or computationally efficient ESPRIT [21] method, no ambiguity and *independent* angle estimate, denoted by $\hat{\alpha}_r$, can be obtained.

Likewise, similar to the estimation process of no ambiguity and *independent* angle α_r, we first compute the two matrices $\mathbf{R}_x$ and $\bar{\mathbf{R}}_x$ similar to (4) and (7) respectively, then construct another Toeplitz matrix $\mathbf{R}_{Tx}$ like $\mathbf{R}_{Ty}$, and finally using the MUSIC or ESPRIT method, no ambiguity and *independent* angle estimate, denoted by $\hat{\beta}_r$, can be obtained.

4. IMPROVED METHOD

Since the proposed method is based on the LSA, thus it has larger array aperture than a ULA when the same number of sensors is used, which indicates that the proposed method with LSA is able to gain a better *independent* angle resolution than the MUSIC or ESPRIT method with ULA.

By simulations, the fact, that the proposed method has a superior angle resolution, has been verified; however, it is found that with the finite samples and SNR, its *independent* angle estimation performance is slightly below the MUSIC and ESPRIT methods.

4.1. First Improved HRNA (FI-HRNA) Method for High Performance DOA Estimation

In order to achieve high performance angle estimation, first improved HRNA method is proposed.

With the LSA on the Y axis, we first use the MUSIC method to obtain all *independent* angles estimates $\{\hat{\alpha}_1, \hat{\alpha}_2, \ldots, \hat{\alpha}_P\}$, which contain one real angle estimate α_r and $P-1$ false angle ones, by one-dimensional (1D) search in interval $(0, \pi]$. Then we extract the fine but no ambiguity and real angle estimate by solving the following constrained optimization problem:

$$\hat{\alpha}_{fr} = \min_{i=1,\ldots,P} (\hat{\alpha}_i - \hat{\alpha}_r)^2 \quad (15)$$

where $\hat{\alpha}_{fr}$ denotes the fine but no ambiguity and real angle estimate.

4.2. Second Improved HRNA (SI-HRNA) Method for Low Computational Load

In order to obtain all *independent* angles estimates $\{\hat{\alpha}_1, \hat{\alpha}_2, \ldots, \hat{\alpha}_P\}$, the first improved HRNA method in Section 4.1 needs to perform 1D search in interval $(0, \pi]$, which will bring out a larger computational cost.

In order to achieve high performance angle estimation and simultaneously decrease the computational load, second improved HRNA method is presented as: **Step 1)** based on the proposed HRNA method in Section 3, obtain the *independent* angle estimate $\hat{\alpha}_r$; **Step 2)** reset a search interval

$[\hat{\alpha}_r - \Delta\alpha, \hat{\alpha}_r + \Delta\alpha]$, where $\Delta\alpha$ is a constant, less than $\pi/2$ and can be adjusted according to the estimation accuracy of angle estimate $\hat{\alpha}_r$; **Step 3)** with the LSA, use the MUSIC method to perform a search in interval $[\hat{\alpha}_r - \Delta\alpha, \hat{\alpha}_r + \Delta\alpha]$ so as to obtain the *independent* angles estimates $\{\hat{\alpha}_1, \hat{\alpha}_2, \ldots, \hat{\alpha}_G\}$ which are close to angle estimate $\hat{\alpha}_r$ and belong to the interval $[\hat{\alpha}_r - \Delta\alpha, \hat{\alpha}_r + \Delta\alpha]$; **Step 4)** similar to (15), use (16) to extract the fine but no ambiguity angle estimate.

$$\hat{\alpha}_{fr} = \min_{i=1,\ldots,G} (\hat{\alpha}_i - \hat{\alpha}_r)^2 \tag{16}$$

On the one hand, the search range $\hat{\alpha}_r + \Delta\alpha - (\hat{\alpha}_r - \Delta\alpha) = 2\Delta\alpha$ of the interval $[\hat{\alpha}_r - \Delta\alpha, \hat{\alpha}_r + \Delta\alpha]$ is much smaller than the search range $\pi - 0 = \pi$ of the interval $(0, \pi)$; on the other hand, the computational load is less than (15) for $G \ll P$; therefore, the SI-HRNA method in Section 4.2 has lower computational cost than the FI-HRNA method in Section 4.1 and the same *independent* angle estimation accuracy as one.

5. SUMMARY OF THE PROPOSED METHODS

The proposed methods can be described as follows: **Step 1):** Construct matrices $\mathbf{R}_{Ty}$ and $\mathbf{R}_{Tx}$ from $\mathbf{R}_y$ and $\mathbf{R}_x$ respectively, and then obtain the *independent* angle estimates $\hat{\alpha}_r$ and $\hat{\beta}_r$ based on $\mathbf{R}_{Ty}$ and $\mathbf{R}_{Tx}$ respectively by utilizing the computationally efficient ESPRIT method. **Step 2):** Determine the small range search intervals $[\hat{\alpha}_r - \Delta\alpha, \hat{\alpha}_r + \Delta\alpha]$ and $[\hat{\beta}_r - \Delta\beta, \hat{\beta}_r + \Delta\beta]$, respectively. **Step 3):** Apply the MUSIC method to matrices $\mathbf{R}_y$ and $\mathbf{R}_x$ respectively, and obtain *independent* angle estimates $\{\hat{\alpha}_1, \hat{\alpha}_2, \ldots, \hat{\alpha}_G\}$ and $\{\hat{\beta}_1, \hat{\beta}_2, \ldots, \hat{\beta}_Q\}$ respectively through 1D search in intervals $[\hat{\alpha}_r - \Delta\alpha, \hat{\alpha}_r + \Delta\alpha]$ and $[\hat{\beta}_r - \Delta\beta, \hat{\beta}_r + \Delta\beta]$, respectively. **Step 4):** According to $\hat{\alpha}_{fr} = \min_{i=1,\ldots,G} (\hat{\alpha}_i - \hat{\alpha}_r)^2$ and $\hat{\beta}_{fr} = \min_{i=1,\ldots,Q} (\hat{\beta}_i - \hat{\beta}_r)^2$ respectively, obtain the *independent*, no ambiguity, fine and real angle estimates $\hat{\alpha}_{fr}$ and $\hat{\beta}_{fr}$. **Step 5):** Based on (5), compute elevation and azimuth angles from independent angle estimates $\hat{\alpha}_{fr}$ and $\hat{\beta}_{fr}$.

6. SIMULATIONS

In this section, to verify the performance of the proposed and its two improved methods, various typical numerical experiments are performed. Since the Joint SVD (JSVD) method in [19] also computes the joint elevation and azimuth angles by first estimating independent angles, thus the proposed methods is compared with both the MUSIC method [18, 22] and JSVD method [19]. The proposed methods uses a L-shaped array placed in the X-Y plane, and each **LSA** branch (see Fig. 2) consists of 6 omni-directional sensors with $d = \lambda/2$; however, the JSVD method and MUSIC method use the L-shaped array placed in the Y-Z and X-Y plane respectively, and their each array branch is **ULA** rather than LSA and consists of 6 omni-directional sensors with $d = \lambda/2$.

In the first experiment, we compare the elevation and azimuth angles estimation performance as SNR changes. The performances of the mentioned methods are measured by estimated root-mean-square error (RMSE) [23, 24] of 500 independent Monte Carlo experiments [25, 26]. The snapshots number is 600, and elevation and azimuth angles are 45° and 120°, respectively. Figs. 4(a)–(b) and 5(a)–(b) show the RMSEs of angles estimates with $D = 5d$ and $D = 16d$, respectively, for the proposed methods, JSVD method [19] and 2D MUSIC method [22].

On the one hand, from Figs. 4(a)–(b), some results can be obtained as: **1)** the proposed HRNA method has the lowest elevation and azimuth angles estimation accuracy, while the 2D MUSIC method in [22] gains better elevation and azimuth angles estimation performance than the HRNA one; this is because the 2D MUSIC method directly utilizes the array covariance matrix to achieve the angles estimation, while the HRNA method needs to use the estimated noise variance $\hat{\sigma}_n$ to form a new covariance matrix-like so as to complete the elevation and azimuth angles estimation; **2)** the JSVD method obtains slightly smaller RMSEs of both elevation and azimuth angles estimates than the 2D MUSIC method, which is consistent with the analysis and results in [19]; **3)** the elevation and azimuth angles estimation accuracy of the SI-HRNA method far exceeds the HRNA, 2D MUSIC and JSVD
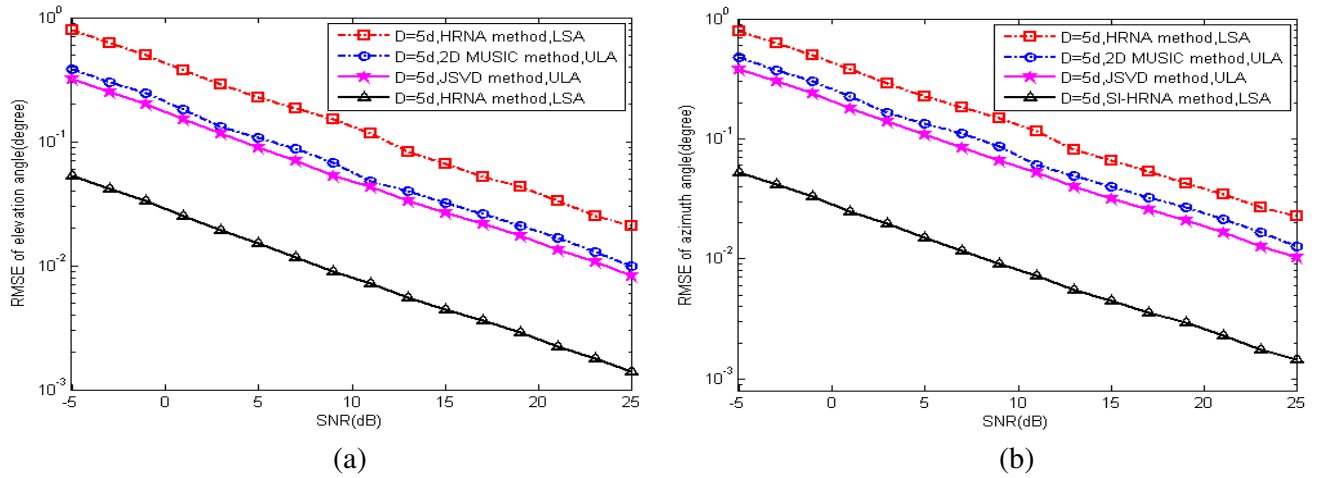
Figure 4. (a) Elevation estimation results with $D = 5d$. (b) Azimuth estimation results with $D = 5d$.
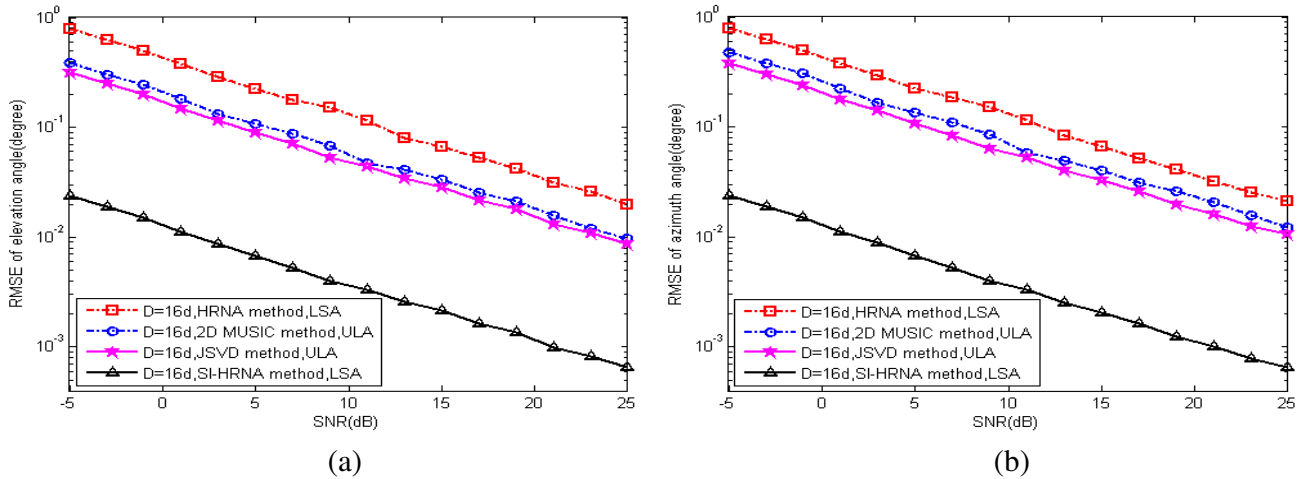

Figure 5. (a) Elevation estimation results with $D = 16d$. (b) Azimuth estimation results with $D = 16d$.

methods, which is because that the SI-HRNA method has much larger array aperture than other three methods; **4)** the elevation angle estimation performance of both the HRNA and SI-HRNA methods is nearly equal to their azimuth angle estimation performance, however, the azimuth angle estimation performance of both 2D MUSIC and JSVD methods is slightly below their elevation angle estimation performance; this is because that both the HRNA and SI-HRNA methods first independently obtain the estimates ($\hat{\alpha}_r$ and $\hat{\beta}_r$) of two *independent* 2D angles (α_r and β_r) using the same computational procedure, and then compute the elevation and azimuth angles by utilizing (5) (in other words, the estimation processes of elevation and azimuth angles are equal and independent with each other), however, the azimuth angle estimates of both 2D MUSIC and JSVD methods are based on their elevation angle ones. On the other hand, comparing Figs. 4(a)–(b) and Figs. 5(a)–(b), one can find that whether $D = 5d$ or $D = 16d$, the elevation and azimuth angles estimation accuracy of the proposed HRNA method changes little, while the proposed SI-HRNA method obtains better elevation and azimuth angles estimation accuracy with $D = 16d$ than that with $D = 5d$. This can be explained that the array aperture with $D = 16d$ is greater than one with $D = 5d$. Therefore, when a very high accuracy angles estimation result is asked and the number of sensors is not allowed to increase, one only needs to adjust the array aperture (namely, the size of k), and thus a higher angles resolution can be obtained accordingly for the large array aperture. Besides, Figs. 4(a)–(b) and Figs. 5(a)–(b) show that even at low SNR, the

proposed SI-HNRA method is able to complete high accuracy elevation and azimuth angles estimation.

In the second experiment, we examine the angles resolution and state the setup process of smaller computational cost search interval $[\hat{\alpha}_r - \Delta\alpha, \ \hat{\alpha}_r + \Delta\alpha]$ and $[\hat{\beta}_r - \Delta\beta, \ \hat{\beta}_r + \Delta\beta]$. Note that in Section 3, we have indicated that the MUSIC or computationally efficient ESPRIT method can be used to the constructed Toeplitz matrices $\mathbf{R}_{Tx}$ or $\mathbf{R}_{Ty}$ so as to obtain no ambiguity and *independent* angles estimates, however, in practical, in order to decrease the computational load, the computationally efficient ESPRIT method is most likely to be chosen. However, in this experiment, to obtain MUSIC spectrum to compare the angles resolution, we use the MUSIC method to estimate no ambiguity and *independent* angles. Moreover, the angles resolution of the proposed HRNA and FI-HRNA methods is compared with the 1D MUSIC method in [18]. Two *independent* angles α_r and β_r are set to 30° and 60°, respectively. The SNR and number of snapshots are set to 0 dB and 500, respectively. The relevant array aperture factor D is set to $D = 16d$. Figs. 6(a)–(b) show that MUSIC angles spectrum of three methods (the HRNA, 2D MUSIC and FI-HRNA methods).
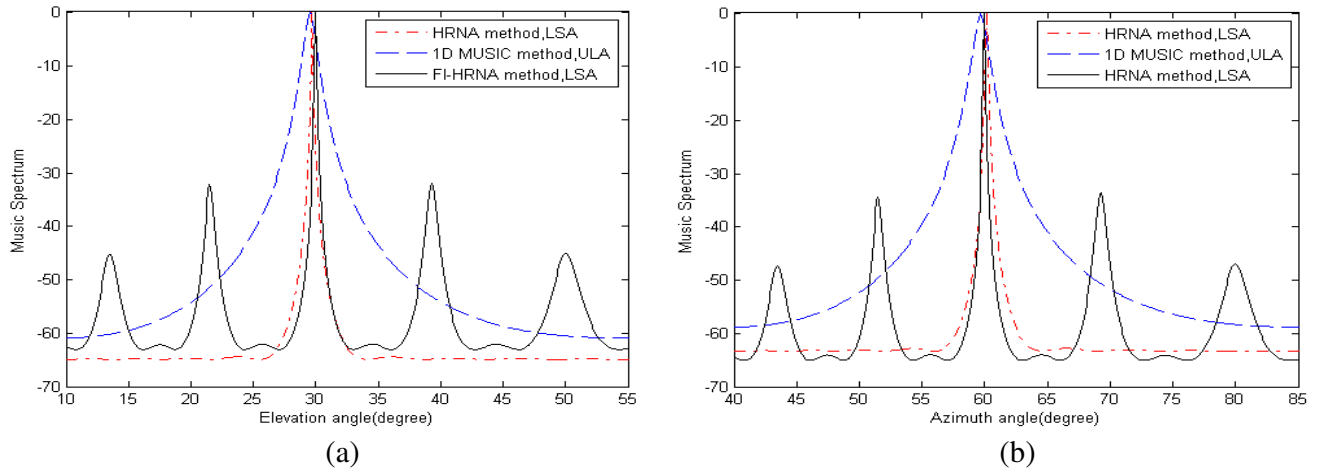

Figure 6. (a) The elevation angle MUSIC spectrum. (b) The azimuth angle MUSIC spectrum.

It can be observed easily from Figs. 6(a)–(b) that the proposed HRNA and FI-HRNA methods with LSA gains higher angles resolution than MUSIC method with ULA, which is because that the proposed HRNA and FI-HRNA methods have larger array aperture than the MUSIC method. More important, since the array aperture of the proposed HRNA and FI-HRNA methods can be adjusted according to practical demand, a very high angles resolution can be achieved when array aperture is very large. In addition, Figs. 6(a)–(b) show that angles estimate of the HRNA method is close to one of the FI-HRNA method, and thus the angles search interval $[\hat{\alpha}_r - \Delta\alpha, \ \hat{\alpha}_r + \Delta\alpha]$ and $[\hat{\beta}_r - \Delta\beta, \ \hat{\beta}_r + \Delta\beta]$ can be set to a very small size, such as $\Delta\alpha = 10°$ and $\Delta\beta = 10°$, which can highly decrease the computational cost for search and the proposed SI-HRNA method is just based on this idea. Moreover, the larger the array aperture is, the smaller the angles search interval can be set to. Finally, comparing Figs. 4(a)–(b), 5(a)–(b) and Figs. 6(a)–(b), one can find that although the angles estimation performance of the proposed HRNA method is lower than the MUSIC method, its angles resolution is superior to the MUSIC method for large array aperture.

7. CONCLUSION

In this paper, based on a two orthogonal LSA, a HRNA and its two improved methods (FI-HRNA and SI-HRNA methods) are proposed to estimate the 2D angles of single source. Although the angles estimation accuracy of the HRNA method is lower than the MUSIC method, its angles resolution is superior to the MUSIC method. The FI-HRNA method overcomes the disadvantage of low angles estimation accuracy, and obtains high angles estimation accuracy and resolution. The SI-HRNA method not only holds the advantage of high angles estimation accuracy and resolution of the FI-HRNA method, but also

highly decreases the computational load. Although based on the sparse array, the proposed HRNA and improved methods is able to automatically overcome angle ambiguity problem of sparse array and the two improved methods (FI-HRNA and SI-HRNA methods) can achieve high angles estimation accuracy and resolution. What's more, when the number of sensors is not allowed to increase, the proposed FI-HRNA and SI-HRNA methods can obtain a desirable angles estimation accuracy and resolution by adjusting the relevant array aperture factor D (namely, adjust the array aperture).

ACKNOWLEDGMENT

REFERENCES

1. Ying, D. W. and Y. H. Yan, "Robust and fast localization of single speech source using a planar array," *IEEE Signal Processing Letters*, Vol. 20, No. 9, 909–912, 2013.
2. Cheung, K. W., H. C. So, W. K. Ma, and Y. T. Chan, "Least squares algorithms for time-of-arrival-based mobile location," *IEEE Transactions on Signal Processing*, Vol. 52, No. 4, 1121–1130, 2004.
3. Stoica, P. and J. Li, "Source localization from range-difference measurements," *IEEE Signal Processing Magazine*, Vol. 23, No. 6, 63–39, 2006.
4. Sayed, A. H, A. Tarighat, and N. Khajehnouri, "Network-based wireless location: Challenges faced in developing techniques for accurate wireless location information," *IEEE Signal Processing Magazine*, Vol. 22, No. 4, 24–40, 2005.
5. Beck, A. and D. Pan, "On the solution of the GPS localization and circle fitting problems," *SIAM J. Optim.*, Vol. 22, No. 1,108–134, 2012.
6. Heidenreich, P., A. M. Zoubir, and M. Rübsamen, "Joint 2-D DOA estimation and phase calibration for uniform rectangular arrays," *IEEE Transactions on Signal Processing*, Vol. 60, No. 9, 4683–4693, 2012.
7. Doroslovacki, M. I. and E. G. Larsson, "Nonuniform linear antenna arrays minimising Cramer-Rao bounds for joint estimation of single source range and direction of arrival," *IEE Proc. — Radar Sonar Navig.*, Vol. 152, No. 4, August 2005.
8. Beck, A., M. Teboulle, and Z. Chikishev, "Iterative minimization schemes for solving the single source localization problem," *SIAM J. Optim.*, Vol. 19, No. 3, 1397–1416, 2008.
9. Reed, J. D, R. M. Buehrer, and C. R. C. M. da Silva, "An optimization approach to single-source localization using direction and range estimates," *IEEE Global Telecommunications Conference*, 1–5, GLOBECOM 2009.
10. Qi, H.-D., N. Xiu, and X. M. Yuan, "A lagrangian dual approach to the single-source localization problem," *IEEE Transactions on Signal Processing*, Vol. 61, No. 15, 3815–3826, August 2013.
11. Jiang, J. C., P. Wei, and L. Gan, "Source location based on independent doublet array," *Electronics Letters*, Vol. 49, No. 14, 2013.
12. Wu, Y. T. and H. C. So, "Simple and accurate two-dimensional angle estimation for a single source with uniform circular array," *IEEE Antennas and Wireless Propagation Letters*, Vol. 7, 78–80, 2008.
13. Liao, B., Y.-T. Wu, and S.-C. Chan, "A generalized algorithm for fast two-dimensional angle estimation of a single source with uniform circular arrays," *IEEE Antennas and Wireless Propagation Letters*, Vol. 11, 984–986, 2012.
14. Bellili, F., S. Affes, and A. Stephenne, "Second-order moment-based direction finding of a single source for ULA systems," *2011 IEEE 22nd International Symposium on Personal Indoor and Mobile Radio Communications (PIMRC)*, 1944–1947, 2011.

15. Bianchi, P., M. Debbah, M. Maida, and J. Najim, "Performance of statistical tests for single-source detection using random matrix theory," *IEEE Transactions on Information Theory*, Vol. 57, No. 4, 2400–2419, 2011.

16. Gazzah, H. and J.-P. Delmas, "Spectral efficiency of beamforming-based parameter estimation in the single source case," *2011 IEEE Statistical Signal Processing Workshop (SSP)*, 153–156, 2011.

17. Yuan, X., "Direction-finding wideband linear FM sources with triangular arrays," *IEEE Transactions on Aerospace and Electronic Systems*, Vol. 48, No. 3, July 2012.

18. Schmidt, R. O., "Multiple emitter location and signal parameters estimation," *IEEE Trans. on Antennas and Propagation*, Vol. 34, No. 3, 267–280, 1986.

19. Gu, J.-F. and P. Wei, "Joint SVD of two cross-correlation matrices to achieve automatic pairing in 2-D angle estimation problems," *IEEE Antennas and Wireless Propagation Letters*, Vol. 6, 553–556, 2007.

20. Bresler, Y., "Maximum likelihood estimation of a linearly structured covariance with application to antenna array processing," *ASSP Workshop on Spectrum Estimation Model.*, 172–175, Minneapolis, 1988.

21. Roy, R. and T. Kailath, "ESPRIT — Estimation of signal parameters via rotational invariance techniques," *IEEE Trans. on Acoust., Speech, Signal Process.*, Vol. 37, 984–995, July 1989.

22. Porozantzidou, M. G. and M. T. Chryssomallis, "Azimuth and elevation angles estimation using 2-D music algorithm with an L-shape antenna," *2010 IEEE Antennas and Propagation Society International Symposium (APSURSI)*, 1–4, July 2010.

23. Jiang, J. J., D. Fajie, and C. Jin, "Three-dimensional localization algorithm for mixed near-field and far-field sources based on ESPRIT and MUSIC method," *Progress In Electromagnetics Research*, Vol. 136, 435–456, 2013.

24. Cheng, S.-C. and K.-C. Lee, "Reducing the array size for DOA estimation by an antenna mode switch technique," *Progress In Electromagnetics Research*, Vol. 131, 117–134, 2012.

25. Liang, J. and D. Liu, "Two L-shaped array-based 2-D DOAs estimation in the presence of mutual coupling," *Progress In Electromagnetics Research*, Vol. 112, 273–298, 2011.

26. Li, Y. and H. Ling, "Improved current decomposition in helical antennas using the ESPRIT algorithm," *Progress In Electromagnetics Research*, Vol. 106, 279–293, 2010.